Table 2. (*Continued*)

Affy ID	Gene name	Symbol	Fold-change
1255_g_at	guanylate cyclase activator 1A	GCAP	0·49559578
222858_s_at	Dual adaptor of phosphotyrosine and 3-phosphoinositides	DAPP1	0·4963491
204730_at	Regulating synaptic membrane exocytosis 3	RIMS3	0·5001501
207826_s_at	Inhibitor of DNA binding 3	ID3	0·50062287
33304_at	Interferon stimulated exonuclease gene 20 kDa	ISG20	0·50399923
211928_at	Dynein, cytoplasmic 1, heavy chain 1	DNCH1	0·5087544
242195_x_at	Numb homolog (Drosophila)-like	NUMBL	0·5093039
209257_s_at	Chondroitin sulfate proteoglycan 6	CSPG6	0·51205146
215990_s_at	B-cell CLL/lymphoma 6	BCL5	0·51233035
227396_at	Protein tyrosine phosphatase, receptor type, J	PTPRJ	0·5157389
228056_s_at	Napsin B aspartic peptidase pseudogene	NAPSB	0·5182605
228787_s_at	Breast carcinoma amplified sequence 4	BCAS4	0·51919734
225327_at	KIAA1370	FLJ10980	0·5194209
212368_at	Zinc finger protein 292	ZNF292	0·5197308
228343_at	POU domain, class 2, transcription factor 2	POU2F2	0·5240128
209138_x_at		IGLJ3	0·52593404
214016_s_at	Splicing factor proline/glutamine-rich	SFPQ	0·5273748
201236_s_at	BTG family, member 2	BTG2	0·5273795
202033_s_at	RB1-inducible coiled-coil 1	RB1CC1	0·5290374
219911_s_at	Solute carrier organic anion transporter family, member 4A1	SLCO4A1	0·5337818
204867_at	GTP cyclohydrolase I feedback regulator	GCHFR	0·53428966
209579_s_at	Methyl-CpG binding domain protein 4	MBD4	0·5378972
207761_s_at	DKFZP586A0522 protein	DKFZP586A0522	0·53842366
219517_at	Elongation factor RNA polymerase II-like 3	ELL3	0·53930795
207339_s_at	Lymphotoxin beta	LTB	0·53969586
228031_at	Hypothetical protein LOC149705	C20orf121	0·5410639
206219_s_at	Vav 1 oncogene	VAV1	0·54299057
231716_at	Membrane associated DNA binding protein	MNAB	0·5447174
213036_x_at	ATPase, Ca++ transporting, ubiquitous	SERCA3	0·5453293
230740_at	Transcribed locus	EHD3	0·5472777
230777_s_at	PR domain containing 15	PRDM15	0·54828
210679_x_at	Homo sapiens cDNA clone MGC:3878 IMAGE:3609162	BCL7A	0·55017775
229147_at	Ras association (RalGDS/AF-6) domain family 6	RASSF6	0·5539612
233746_x_at	Huntingtin interacting protein K	HYPK	0·55896664
224616_at	Dynein, cytoplasmic 1, light intermediate chain 2	DNCLI2	0·5595679
212677_s_at	RAB1A, member RAS oncogene family	RAB1A	0·5602901
213016_at	Bobby sox homolog	BBX	0·56184375
211383_s_at	WD repeat domain 37	WDR37	0·56346995
215504_x_at	Ankyrin repeat domain 10	ANKRD10	0·563754
212119_at	602149641F1 NIH_MGC_81	RHOQ	0·5639594
203819_s_at	IGF-II mRNA-binding protein 3	IMP-3	0·5641141
205124_at	MADS box transcription enhancer factor 2, polypeptide B	MEF2B	0·56775457
220071_x_at	Centrosomal protein 27 kDa	C15orf25	0·56932724
219396_s_at	Nei endonuclease VIII-like 1	NEIL1	0·5707603
226372_at	Carbohydrate (chondroitin 4) sulfotransferase 11	CHST11	0·57161444
232266_x_at	Homo sapiens cDNA FLJ14317 fis, clone PLACE3000401.	CDC2L5	0·57188374
211445_x_at	Nascent-polypeptide-associated complex alpha polypeptide pseudogene 1	FKSG17	0·5727707
224829_at	Cytoplasmic polyadenylation element binding protein 4	CPEB4	0·57316726
229353_s_at	Nuclear casein kinase and cyclin-dependent kinase substrate 1	NUCKS	0·5739766
215457_at	Actin related protein 2/3 complex, subunit 1A, 41 kDa	ARPC1A	0·5758453
1569594_a_at	Serologically defined colon cancer antigen 1	SDCCAG1	0·5770196
200596_s_at	Eukaryotic translation initiation factor 3, subunit 10 theta, 150/170 kDa	EIF3S10	0·5771801
209023_s_at	Stromal antigen 2	STAG2	0·57891893
203140_at	B-cell CLL/lymphoma 6	BCL6	0·5807235
217862_at	Protein inhibitor of activated STAT, 1	PIAS1	0·5808474

Table 2. (*Continued*)

Affy ID	Gene name	Symbol	Fold-change
227748_at	RNA binding motif protein, X-linked-like 1	KAT3	0·5812906
229429_x_at	LOC440667		0·582004
227740_at	U2AF homology motif (UHM) kinase 1	UHMK1	0·5825476
208615_s_at	Protein tyrosine phosphatase type IVA, member 2	PTP4A2	0·58321685
209360_s_at	Runt-related transcription factor 1	RUNX1	0·58370924
213734_at	WD repeat and SOCS box-containing 2	WSB2	0·5844417
202996_at	Polymerase (DNA-directed), delta 4	POLD4	0·58979243
212047_s_at	Ring finger protein 167	RNF167	0·59118843
218886_at	PAK1 interacting protein 1	PAK1IP1	0·59172606
215179_x_at	Placental growth factor	PGF	0·59284484
204141_at	Tubulin, beta 2A	TUBB2	0·5932073
212810_s_at	Solute carrier family 1, member 4	SLC1A4	0·59446627
201193_at	Isocitrate dehydrogenase 1 (NADP+), soluble	IDH1	0·59564257
228153_at	IBR domain containing 2	IBRDC2	0·59580594
64418_at	AP1 gamma subunit binding protein 1	AP1GBP1	0·5966325
203143_s_at	Transcribed locus	KIAA0040	0·5968683
209076_s_at	WDR45-like	WDR45L	0·5985668
204076_at	Ectonucleoside triphosphate diphosphohydrolase 4	ENTPD4	0·59857833
1558080_s_at	Hypothetical protein LOC144871	DNAJC3	0·5994704
203044_at	Carbohydrate (chondroitin) synthase 1	CHSY1	0·60100013
234762_x_at	Neurolysin (metallopeptidase M3 family)	NLN	0·6012079
207124_s_at	Guanine nucleotide binding protein (G protein), beta 5	GNB5	0·6012481
204449_at	Phosducin-like	PDCL	0·6038013
226508_at	Polyhomeotic like 3 (Drosophila)	PHC3	0·60685164
204681_s_at	Rap guanine nucleotide exchange factor (GEF) 5	RAPGEF5	0·60706514
203346_s_at	Metal response element binding transcription factor 2	M96	0·6077221
200998_s_at	Cytoskeleton-associated protein 4	CKAP4	0·608657
222816_s_at	Zinc finger, CCHC domain containing 2	ZCCHC2	0·6087468
219158_s_at	Synonyms: Ga19, NAT1, NATH, TBDN100	NARG1	0·6090036
201901_s_at	YY1 transcription factor	YY1	0·6101737
229072_at	RAB30, member RAS oncogene family	RAB30	0·6116257
212604_at	Mitochondrial ribosomal protein S31	MRPS31	0·61232865
214352_s_at	V-Ki-ras2 Kirsten rat sarcoma viral oncogene homolog	KRAS2	0·6126175
231825_x_at	Activating transcription factor 7 interacting protein	ATF7IP	0·6132226
225204_at	T-cell activation protein phosphatase 2C	TA-PP2C	0·6143749
202379_s_at	Natural killer-tumor recognition sequence	NKTR	0·61503386
204853_at	Origin recognition complex, subunit 2-like	ORC2L	0·6158861
201138_s_at	Sjogren syndrome antigen B	SSB	0·6166977
225136_at	Pleckstrin homology domain containing, family A, member 2	PLEKHA2	0·6169427
201384_s_at	Neighbor of BRCA1 gene 1	M17S2	0·61722594
213620_s_at	Intercellular adhesion molecule 2	ICAM2	0·61761326
226158_at	Kelch-like 24	DRE1	0·6183106
205383_s_at	Zinc finger and BTB domain containing 20	ZBTB20	0·62210584
219148_at	PDZ binding kinase	PBK	0·6229036
227402_s_at	Chromosome 8 open reading frame 53	MGC14595	0·6240476
206641_at	Tumor necrosis factor receptor superfamily, member 17	TNFRSF17	0·62757266
202412_s_at	Ubiquitin specific peptidase 1	USP1	0·6286277
227224_at	Ral GEF with PH domain and SH3 binding motif 2	RALGPS2	0·62964123
231809_x_at	EST365840 MAGE resequences, MAGC	PDCD7	0·6322018
200797_s_at	Myeloid cell leukemia sequence 1	MCL1	0·6327875
204912_at	Interleukin 10 receptor, alpha	IL10RA	0·63407373
210754_s_at	V-yes-1 Yamaguchi sarcoma viral related oncogene homolog	LYN	0·6343251
235469_at	Similar to RIKEN cDNA 5830415L20	MGC40405	0·6344833
208415_x_at	Inhibitor of growth family, member 1	ING1	0·6353071
229656_s_at	Similar to echinoderm microtubule associated protein like 5		0·6356807

Table 2. (*Continued*)

Affy ID	Gene name	Symbol	Fold-change
224875_at	Hypothetical protein FLJ37562	FLJ37562	0·6361133
230110_at	Mucolipin 2	MCOLN2	0·6363045
213502_x_at	Similar to bK246H3·1	LOC91316	0·63717055
209272_at	NGFI-A binding protein 1	NAB1	0·6376612
214677_x_at	Immunoglobulin lambda joining 3	IGLC2	0·6377649
220999_s_at	synonym: PIR121; p53 inducible protein	CYFIP2	0·6382754
201320_at	SWI/SNF related, matrix associated, actin dependent regulator of chromatin	SMARCC2	0·63914317
223553_s_at	Docking protein 3	DOK3	0·63973147
214730_s_at	Golgi apparatus protein 1	GLG1	0·64044565
1555989_at	Dishevelled associated activator of morphogenesis 1	DAAM1	0·641099
210142_x_at	Flotillin 1	FLOT1	0·64127034
228098_s_at	Myosin regulatory light chain interacting protein	MYLIP	0·6423752
226464_at	Hypothetical protein MGC33365	MGC33365	0·64265686
227189_at	Copine V	CPNE5	0·64277476
228910_at	CD82 antigen	KAI1	0·643213
208246_x_at	hypothetical protein FLJ20006	FLJ20006	0·64384246
1565627_a_at	Leucine-rich repeat kinase 1	LRRK1	0·6438542
208070_s_at	REV3-like, catalytic subunit of DNA polymerase zeta	REV3L	0·64388376
226779_at	LMBR1 domain containing 2	DKFZp434H2226	0·64402026
212760_at	Ubiquitin protein ligase E3 component n-recognin 2	UBR2	0·6447363
232644_x_at	OCIA domain containing 1	OCIAD1	0·6447408
205922_at	Vanin 2	VNN2	0·6448793
209062_x_at	Nuclear receptor coactivator 3	NCOA3	0·64496595
200842_s_at	Glutamyl-prolyl-tRNA synthetase	EPRS	0·645458
212733_at	KIAA0226	KIAA0226	0·64567864
244887_at	Regulator of G-protein signalling 13	RGS13	0·6465569
205370_x_at	Dihydrolipoamide branched chain transacylase E2	DBT	0·6465768
219812_at	Stromal antigen 3	MGC2463	0·64680105
202378_s_at	Leptin receptor	LEPR	0·6468874
204285_s_at	Phorbol-12-myristate-13-acetate-induced protein 1	PMAIP1	0·6495961
228151_at	Transcribed locus		0·6497464
213007_at	KIAA1794	FLJ10719	0·6498637
222891_s_at	B-cell CLL/lymphoma 11A	BCL11A	0·64996225
220085_at	Helicase, lymphoid-specific	HELLS	0·6502575
220746_s_at	Receptor associated protein 80	RAP80	0·65041715
213111_at	Phosphatidylinositol-3-phosphate/phosphatidylinositol 5-kinase, type III	PIP5K3	0·65109867
203318_s_at	Zinc finger protein 148	ZNF148	0·6520053
202655_at	Arginine-rich, mutated in early stage tumors	ARMET	0·6522758
225273_at	KIAA1280 protein	KIAA1280	0·6529812
204709_s_at	Kinesin family member 23	KIF23	0·65339863
218358_at	Cysteine-rich with EGF-like domains 2	MGC11256	0·6534136
201917_s_at	Solute carrier family 25, member 36	FLJ10618	0·65368974
220933_s_at	Zinc finger, CCHC domain containing 6	ZCCHC6	0·6548457
212588_at	Protein tyrosine phosphatase, receptor type, C	PTPRC	0·6555439
215780_s_at	Human DNA sequence from clone RP1-30P20	SET	0·65566504
239748_x_at	yl95h12.s1 Soares infant brain 1NIB		0·6571978
209780_at	Putative homeodomain transcription factor 2	PHTF2	0·65742826
211040_x_at	G-2 and S-phase expressed 1	GTSE1	0·659053
206150_at	TAP binding protein-like	TNFRSF7	0·6612941
209049_s_at		PRKCBP1	0·66141385
217796_s_at	Nuclear protein localization 4	NPL4	0·6618553
222737_s_at	Bromodomain containing 7	BRD7	0·6626274
218306_s_at	Hect domain and RCC1 (CHC1)-like domain (RLD) 1	HERC1	0·662763
222420_s_at	Ubiquitin-conjugating enzyme E2H	UBE2H	0·66321975
210962_s_at	A kinase (PRKA) anchor protein (yotiao) 9	AKAP9	0·6633441

Table 2. (*Continued*)

Affy ID	Gene name	Symbol	Fold-change
1555275_a_at	Kelch-like 6 (Drosophila)	KLHL6	0·6639439
218348_s_at	Zinc finger CCCH-type containing 7A	ZC3HDC7	0·6641935
233329_s_at	Hypothetical protein LOC51315	LOC51315	0·66421455
225232_at	Myotubularin related protein 12	PIP3AP	0·66434306
230917_at	CDNA FLJ45450 fis, clone BRSTN2002691		0·664679
202181_at	KIAA0247	KIAA0247	0·66494757
210561_s_at	WD repeat and SOCS box-containing 1	WSB1	0·66532546
206272_at	S-phase response (cyclin-related)	SPHAR	0·66562426
201498_at	Ubiquitin specific peptidase 7 (herpes virus-associated)	USP7	0·6661961
235661_at	ye65a03.r1 Soares fetal liver spleen 1NFLS		0·666862
228087_at	LOC90693 protein	LOC90693	0·6674958
218150_at	ADP-ribosylation factor-like 5A	ARL5	0·6685538
203608_at		ALDH5A1	0·6689315
213460_x_at	Williams Beuren syndrome chromosome region 20C	WBSCR20C	0·6701285
202922_at	Glutamate-cysteine ligase, catalytic subunit	GCLC	0·67089856
222408_s_at	Yippee-like 5	YPEL5	0·671024
223391_at	Sphingosine-1-phosphate phosphatase 1	SGPP1	0·67116857
213166_x_at	Hypothetical protein FLJ14346	FLJ14346	0·67121977
219119_at	LSM8 homolog, U6 small nuclear RNA associated	LSM8	0·67156994
203297_s_at	Jumonji, AT rich interactive domain 2	JARID2	0·67171353
213940_s_at	Formin binding protein 1	FNBP1	0·67211777
224677_x_at	Chromosome 11 open reading frame 31	C11orf31	0·6722119
212066_s_at	Ubiquitin specific peptidase 34	USP34	0·67282677
201779_s_at	Ring finger protein 13	RNF13	0·67283076
243798_at	B-cell CLL/lymphoma 9-like	BCL9L	0·6730866
212023_s_at	Antigen identified by monoclonal antibody Ki-67	MKI67	0·673758
219502_at	Nei endonuclease VIII-like 3	FLJ10858	0·67435133
203556_at	Zinc fingers and homeoboxes 2	ZHX2	0·67446464
237475_x_at	qb48d05.x1 NCI_CGAP_Brn23		0·6744719
202704_at	Transducer of ERBB2, 1	TOB1	0·67514235
225701_at	AT-hook transcription factor	AKNA	0·6767782
219392_x_at	Proline rich 11	FLJ11029	0·67691547
205297_s_at	CD79B antigen	CD79B	0·67695534
226398_s_at	Chromosome 10 open reading frame 4	C10orf4	0·6774105
213064_at	Nuclear protein UKp68	FLJ11806	0·6776265
1559436_x_at	Arrestin, beta 2	ARRB2	0·67766494
212167_s_at	SWI/SNF related, matrix associated, actin dependent regulator of chromatin	SMARCB1	0·6779144
223268_at	LP4947	PTD012	0·6783802
217781_s_at	Zinc finger protein 106 homolog	ZFP106	0·6795011
1556059_s_at	Spen homolog, transcriptional regulator	SPEN	0·6800467
1552448_a_at	Homo sapiens chromosome 8 open reading frame 12 (C8orf12), mRNA.	C8orf12	0·6807321
224602_at	HCV F-transactivated protein 1	LOC401152	0·6808058
212944_at	Mitochondrial ribosomal protein S6	MRPS6	0·6811207
208737_at	ATPase, H+ transporting, lysosomal 13 kDa, V1 subunit G isoform 1	ATP6V1G1	0·6811667
211997_x_at	H3 histone, family 3B	H3F3B	0·68119144
212622_at	Transmembrane protein 41B	KIAA0033	0·68157566
203301_s_at	Cyclin D binding myb-like transcription factor 1	DMTF1	0·68273085
208899_x_at	ATPase, H+ transporting, lysosomal 34 kDa, V1 subunit D	ATP6V1D	0·6829173
202983_at	SWI/SNF related, matrix associated, actin dependent regulator of chromatin	SMARCA3	0·6829173
209250_at	Degenerative spermatocyte homolog 1, lipid desaturase	DEGS1	0·6831875
204581_at	CD22 antigen	CD22	0·6840824
225433_at	General transcription factor IIA, 1, 19/37 kDa	GTF2A1	0·685833
219076_s_at	Peroxisomal membrane protein 2, 22 kDa	PXMP2	0·6862011
208772_at	Ankyrin repeat and KH domain containing 1	ANKHD1	0·68652916
212571_at	Chromodomain helicase DNA binding protein 8	CHD8	0·68715703

Table 2. (*Continued*)

Affy ID	Gene name	Symbol	Fold-change
200920_s_at	B-cell translocation gene 1, anti-proliferative	BTG1	0·6878364
212126_at	Chromobox homolog 5	CBX5	0·687962
203752_s_at	Jun D proto-oncogene	JUND	0·68797
210105_s_at	FYN oncogene related to SRC, FGR, YES	FYN	0·68825364
221501_x_at	Hypothetical protein LOC339047	LOC339047	0·6883818
227696_at	Exosome component 6	EXOSC6	0·688953
201810_s_at	SH3-domain binding protein 5	SH3BP5	0·6889935
206513_at	Absent in melanoma 2	AIM2	0·689059
205484_at	Signaling threshold regulating transmembrane adaptor 1	SIT	0·68912697
225890_at	Chromosome 20 open reading frame 72	C20orf72	0·69149476
213154_s_at	Bicaudal D homolog 2	BICD2	0·6923916
217717_s_at	Tyrosine 3-monooxygenase/tryptophan 5-monooxygenase activation protein	YWHAB	0·69240123
212350_at	TBC1 domain family, member 1	TBC1D1	0·69268274
213128_s_at	Ubiquitin protein ligase E3A	UBE3A	0·6931148
212943_at	KIAA0528 gene product	KIAA0528	0·6943166
203434_s_at	Membrane metallo-endopeptidase	MME	0·69480205
232515_at	Ankyrin repeat and SOCS box-containing 3	ASB3	0·69493157
234984_at	Neural precursor cell expressed, developmentally down-regulated 1	NEDD1	0·6951
204446_s_at	Arachidonate 5-lipoxygenase	ALOX5	0·6954707
221918_at	PCTAIRE protein kinase 2	PCTK2	0·6954857
218384_at	Calcium regulated heat stable protein 1, 24 kDa	CARHSP1	0·6965451
223022_s_at	Chromosome 6 open reading frame 55	C6orf55	0·69656706
217249_x_at	Cytochrome c oxidase subunit VIIa pseudogene 2	COX7A3H	0·69701755
243539_at	Ring finger protein 11	RNF11	0·69720584
210592_s_at	Spermidine/spermine N1-acetyltransferase	SAT	0·69809985
217967_s_at	Chromosome 1 open reading frame 24	C1orf24	0·6989367
228006_at	Phosphatase and tensin homolog	PTEN	0·6992462
204710_s_at	WD repeat domain, phosphoinositide interacting 2	WIPI-2	0·699294
202760_s_at	Paralemmin 2	PALM2-AKAP2	0·6998125
204872_at	Transducin-like enhancer of split 4	TLE4	0·6999074
233702_x_at	Homo sapiens cDNA: FLJ20946 fis, clone ADSE01819.		0·70036465
222986_s_at	Scotin	SCOTIN	0·70078844
223445_at	Dystrobrevin binding protein 1	DTNBP1	0·7017351
203007_x_at	Lysophospholipase I	LYPLA1	0·7029054
235333_at	UDP-Gal:betaGlcNAc beta 1,4- galactosyltransferase, polypeptide 6	B4GALT6	0·7029247
213729_at	Formin binding protein 3	FNBP3	0·70293915
227124_at	MRNA full length insert cDNA clone EUROIMAGE 966164		0·70326364
205733_at	Bloom syndrome	BLM	0·7036139
219304_s_at	Platelet derived growth factor D	PDGFD	0·7036207
219237_s_at	DnaJ (Hsp40) homolog, subfamily B, member 14	FLJ14281	0·7041835
209358_at	TAF11 RNA polymerase II	TAF11	0·7044149
225545_at	Eukaryotic elongation factor-2 kinase	EEF2K	0·70445967
208146_s_at	Carboxypeptidase, vitellogenic-like	CPVL	0·7045879
210972_x_at	T-cell receptor rearranged alpha-chain V-region	TCRA	0·7055038
208579_x_at	H2B histone family, member S	H2BFS	0·7060805
212263_at	Quaking homolog, KH domain RNA binding	QKI	0·707485
202386_s_at	Limkain b1	LKAP	0·7075946
202113_s_at	sorting nexin 2	TRG-9	0·70800734
206323_x_at	Oligophrenin 1	OPHN1	0·70812446
202664_at	Wiskott-Aldrich syndrome protein interacting protein	WASPIP	0·70844746
233093_s_at	Baculoviral IAP repeat-containing 6	BIRC6	0·7087636
218662_s_at	Chromosome condensation protein G	HCAP-G	0·70939666
214508_x_at	CAMP responsive element modulator	CREM	0·7095808
213737_x_at	Transcribed locus	DKFZp434P162	0·7103367
201877_s_at	Protein phosphatase 2, regulatory subunit B (B56), gamma isoform	PPP2R5C	0·7103621

Table 2. (*Continued*)

Affy ID	Gene name	Symbol	Fold-change
212693_at	MDN1, midasin homolog (yeast)	MDN1	0·7104688
212314_at	KIAA0746 protein	KIAA0746	0·71076244
201247_at	Sterol regulatory element binding transcription factor 2	SREBF2	0·7107886
227993_at	Methionyl aminopeptidase 2	METAP2	0·7108942
216508_x_at	similar to nonhistone chromosomal protein HMG-1	WUGSC	0·71091264
227833_s_at	Methyl-CpG binding domain protein 6	MBD6	0·71103483
1566509_s_at	F-box protein 9	FBX9	0·7116769
203279_at	ER degradation enhancer, mannosidase alpha-like 1	EDEM1	0·7119141
235372_at	Fc receptor-like and mucin-like 1	FREB	0·71208745
241968_at	Transcribed locus		0·71281445
206296_x_at	Mitogen-activated protein kinase kinase kinase kinase 1	MAP4K1	0·7130861
212462_at	MYST histone acetyltransferase (monocytic leukemia) 4	MYST4	0·713116
233665_x_at	Mitochondrial translation optimization 1 homolog	MTO1	0·7134478
212209_at	Thyroid hormone receptor associated protein 2	THRAP2	0·7144091
235327_x_at	602284688F1 NIH_MGC_86	UBXD4	0·7144813
230618_s_at	BAT2 domain containing 1	XTP2	0·71461946
236641_at	Kinesin family member 14	KIF14	0·71463937
204224_s_at	GTP cyclohydrolase 1	GCH1	0·7147643
204531_s_at	Breast cancer 1, early onset	BRCA1	0·71507436
203787_at	Single-stranded DNA binding protein 2	SSBP2	0·7154888
212492_s_at	Jumonji domain containing 2B	JMJD2B	0·7159365
202817_s_at	Synovial sarcoma translocation, chromosome 18	SS18	0·7160071
212420_at	E74-like factor 1	ELF1	0·71618116
203338_at	Protein phosphatase 2, regulatory subunit B (B56), epsilon isoform	PPP2R5E	0·7164281
207540_s_at	Spleen tyrosine kinase	SYK	0·71644425
229943_at	Ret finger protein 2	RFP2	0·71658355
218671_s_at	ATPase inhibitory factor 1	ATPIF1	0·71663755
232909_s_at	Fetal Alzheimer antigen	FALZ	0·7174373
225816_at	PHD finger protein 17	PHF17	0·7179169
211713_x_at	KIAA0101	KIAA0101	0·71805906
229394_s_at	Glucocorticoid receptor DNA binding factor 1	GRLF1	0·71806455
212572_at	Serine/threonine kinase 38 like	STK38L	0·71829355
209382_at	Polymerase (RNA) III	POLR3C	0·7190526
225913_at	KIAA2002 protein	KIAA2002	0·7191407
210776_x_at	Transcription factor 3	TCF3	0·7192611
223053_x_at	Ssu72 RNA polymerase II CTD phosphatase homolog	HSPC182	0·71963733
226297_at	Homeodomain interacting protein kinase 3	HIPK3	0·7197105
1558801_at	Nicotinamide nucleotide transhydrogenase	NNT	0·71974134
222369_at	Hypothetical protein FLJ13848	FLJ13848	0·71995664
230352_at	Phosphoribosyl pyrophosphate synthetase 2	PRPS2	0·7200596
202365_at	Hypothetical protein MGC5139	MGC5139	0·7206042
205902_at	Potassium intermediate/small conductance calcium-activated channel	KCNN3	0·72095835
233936_s_at	Zinc finger protein 403	DIF3	0·7217099
201319_at	Myosin regulatory light chain MRCL3	MRCL3	0·72199404
229582_at	Chromosome 18 open reading frame 37	C18orf37	0·7221231
204115_at	Guanine nucleotide binding protein (G protein), gamma 11	GNG11	0·7221238
212010_s_at	Hypothetical protein H41	H41	0·7224393
218421_at	Ceramide kinase	CERK	0·722603
221500_s_at	Syntaxin 16	STX16	0·7226911
222433_at	Enabled homolog	ENAH	0·72285813
211936_at	Heat shock 70 kDa protein 5	HSPA5	0·7232242
203136_at	Rab acceptor 1	RABAC1	0·7233282
209902_at	Ataxia telangiectasia and Rad3 related	ATR	0·7234323
212780_at	Son of sevenless homolog 1	SOS1	0·723696
211503_s_at	RAB14, member RAS oncogene family	RAB14	0·72393346

Table 2. (*Continued*)

Affy ID	Gene name	Symbol	Fold-change
204174_at	Arachidonate 5-lipoxygenase-activating protein	ALOX5AP	0·7239532
223090_x_at	Transmembrane protein vezatin	VEZATIN	0·72426665
226392_at	RAS p21 protein activator 2	RASA2	0·7243885
227990_at	Step II splicing factor SLU7	SLU7	0·72443694
218823_s_at	Potassium channel tetramerisation domain containing 9	KCTD9	0·7246428
202804_at	ATP-binding cassette, sub-family C (CFTR/MRP), member 1	ABCC1	0·7248081
227808_at	DnaJ (Hsp40) homolog, subfamily C, member 15	DNAJD1	0·7252901
208798_x_at	Golgi autoantigen, golgin subfamily a, 8A	GOLGIN-67	0·72628635
213292_s_at	Sorting nexin 13	SNX13	0·72653073
222996_s_at	CXXC finger 5	CXXC5	0·72690076
201237_at	Capping protein (actin filament) muscle Z-line, alpha 2	CAPZA2	0·7269243
224990_at	Hypothetical protein LOC201895	LOC201895	0·72730917
232008_s_at	Bobby sox homolog	BBX	0·7273624
225951_s_at	LOC440309	CHD2	0·727875
213005_s_at	Ankyrin repeat domain 15	ANKRD15	0·72830474
213385_at	Chimerin (chimaerin) 2	CHN2	0·72833586
212952_at	Calreticulin	CALR	0·72959316
219356_s_at	Chromatin modifying protein 5	SNF7DC2	0·7297071
215785_s_at	Cytoplasmic FMR1 interacting protein 2	CYFIP2	0·7301472
227167_s_at	Mesenchymal stem cell protein DSC96		0·73024756
204951_at	Ras homolog gene family, member H	RHOH	0·7306572
229050_s_at	Hypothetical protein MGC16037	MGC16037	0·73081815
224778_s_at	TAO kinase 1	TAOK1	0·7310451
218191_s_at	LMBR1 domain containing 1	C6orf209	0·7311856
200728_at	ARP2 actin-related protein 2 homolog	ACTR2	0·7312589
228959_at	CDNA		0·73128814
224827_at	Dendritic cell-derived ubiquitin-like protein	DC-UbP	0·73133826
218478_s_at	Zinc finger, CCHC domain containing 8	ZCCHC8	0·732107
201864_at	GDP dissociation inhibitor 1	GDI1	0·7322083
212069_s_at	KIAA0515	KIAA0515	0·73250145
202769_at	Cyclin G2	CCNG2	0·7329358
221751_at	Solute carrier family 2, member 3 pseudogene 1	PANK3	0·7336308
223054_at	DnaJ (Hsp40) homolog, subfamily B, member 11	DNAJB11	0·73389965
208765_s_at	Heterogeneous nuclear ribonucleoprotein R	HNRPR	0·7345736
212080_at	Similar to CDNA sequence BC021608	LOC143941	0·73511535
212838_at	Dynamin binding protein	DNMBP	0·73558724
243910_x_at	Cullin-associated and neddylation-dissociated 1	TIP120A	0·73592746
205034_at	Cyclin E2	CCNE2	0·7360657
205267_at	POU domain, class 2, associating factor 1	POU2AF1	0·7366251
202108_at	Peptidase D	PEPD	0·7367287
205367_at	Adaptor protein with pleckstrin homology and src homology 2 domains	APS	0·7371733
1562836_at	DEAD (Asp-Glu-Ala-Asp) box polypeptide 6	DDX6	0·73732203
217823_s_at	Ubiquitin-conjugating enzyme E2, J1	UBE2J1	0·7376396
204658_at	Transformer-2 alpha	TRA2A	0·7381278
225893_at	MRNA; cDNA DKFZp686D04119		0·73877865
226874_at	Kelch-like 8 (Drosophila)	KLHL8	0·73884803
217118_s_at	Chromosome 22 open reading frame 9	C22orf9	0·7391449
209463_s_at	TAF12 RNA polymerase II	TAF12	0·73976564
226134_s_at	Musashi homolog 2	MSI2	0·7397834
1553906_s_at	FYVE, RhoGEF and PH domain containing 2	FGD2	0·739792
209748_at	Spastin	SPG4	0·7398436
212995_x_at	Hypothetical protein FLJ14346	FLJ14346	0·7402725
200967_at	Peptidylprolyl isomerase B	PPIB	0·74033284
204391_x_at	Tripartite motif-containing 24	TIF1	0·74084216
221520_s_at	Cell division cycle associated 8	CDCA8	0·7408515

Table 2. (*Continued*)

Affy ID	Gene name	Symbol	Fold-change
223059_s_at	Chromosome 10 open reading frame 45	C10orf45	0·7411011
224890_s_at	Similar to CG14977-PA	LOC389541	0·7412293
206061_s_at	Dicer1, Dcr-1 homolog	DICER1	0·74136984
201885_s_at	Cytochrome b5 reductase 3	DIA1	0·74161553
212665_at	TCDD-inducible poly(ADP-ribose) polymerase	TIPARP	0·74172264
201242_s_at	ATPase, Na+/K+ transporting, beta 1 polypeptide	ATP1B1	0·74187577
218167_at	Archaemetzincins-2	LOC51321	0·7419247
214715_x_at	Zinc finger protein 160	ZNF160	0·7425452
200654_at	Procollagen-proline, 2-oxoglutarate 4-dioxygenase, beta polypeptide	P4HB	0·74279094
202171_at	Zinc finger protein 161	ZNF161	0·7429878
224250_s_at	SECIS binding protein 2	SECISBP2	0·7430157
222673_x_at	Similar to hypothetical protein MGC17347	LOC159090	0·74343455
1557961_s_at	602536302F1 NIH_MGC_59		0·7434646
202660_at	Family with sequence similarity 20, member C	ITPR2	0·7436526
217901_at	Desmoglein 2	DSG2	0·7440809
222691_at	solute carrier family 35, member B3	CGI-19	0·7441896
205739_x_at	Zinc finger protein 588	ZNF588	0·74437064
224415_s_at	Histidine triad nucleotide binding protein 2	HINT2	0·7444139
209898_x_at	Intersectin 2	ITSN2	0·74446803
203660_s_at	Pericentrin (kendrin)	PCNT2	0·74484545
203947_at	Hypothetical protein LOC283267	CSTF3	0·74533767
212382_at	Transcription factor 4	TCF4	0·7455324
212560_at	Chromosome 11 open reading frame 32	SORL1	0·7456149
218095_s_at	TPA regulated locus	TPARL	0·74569106
216187_x_at	Kinesin 2	KNS2	0·74619925
224599_at	CGG triplet repeat binding protein 1	CGGBP1	0·74662995
230795_at	Histone H4/o	HIST2H4	0·74673605
201266_at	Thioredoxin reductase 1	TXNRD1	0·7467521
201195_s_at	Solute carrier family 7, member 5	SLC7A5	0·74680513
221760_at	Mannosidase, alpha, class 1A, member 1	MAN1A1	0·7468957
225285_at	Branched chain aminotransferase 1, cytosolic	BCAT1	0·747043
217776_at	Retinol dehydrogenase 11	RDH11	0·7471061
219259_at	semaphorin 4A	SEMA4A	0·74722433
223165_s_at	Inositol hexaphosphate kinase 2	IHPK2	0·74733293
201791_s_at	7-dehydrocholesterol reductase	DHCR7	0·74754477
208993_s_at	Peptidyl-prolyl isomerase G	PPIG	0·7477576
202951_at	Serine/threonine kinase 38	STK38	0·7478889
203648_at	TatD DNase domain containing 2	TATDN2	0·74821633
202716_at	Protein tyrosine phosphatase, non-receptor type 1	PTPN1	0·74856865
227601_at	KIAA1627 protein	KIAA1627	0·74859655
204028_s_at	RAB GTPase activating protein 1	RABGAP1	0·74878204
209539_at	Rac/Cdc42 guanine nucleotide exchange factor (GEF) 6	ARHGEF6	0·7491753
202027_at	Chromosome 22 open reading frame 5	C22orf5	0·74919754
1555762_s_at	Megakaryoblastic leukemia 1	MKL1	0·7492855
212205_at	H2A histone family, member V	H2AFV	0·7496612
219553_at	Non-metastatic cells 7, protein expressed in	NME7	0·7496923
208723_at	Ubiquitin specific peptidase 11	USP11	0·749806
222499_at	SIL1 homolog, endoplasmic reticulum chaperone	SIL1	0·74986565

Next we examined the effect of CD40 stimulation on apoptosis induction in MLMA cells. As shown in Fig. 6(b), when CD40 was stimulated by the addition of CD40-ligand (CD40L) in the presence of interleukin-4, induction of apoptosis in MLMA cells was mediated by both BCR- and CD20-cross-linking. Furthermore, when both CD40 and BAFF were simultaneously stimulated, better inhibition of BCR-induced and CD20-induced apoptosis was observed than those mediated by each of them alone.

Discussion

In the present study, we have clearly shown that BAFF can inhibit apoptosis mediated by BCR or CD20 in MLMA cells that exhibit a mature B-cell phenotype. The BCR is thought to play a crucial role in clonal selection and clonal expansion in the process of B-cell development to expand high-affinity clones against exogenous antigens and eliminate self-acting or low-affinity clones.[31] Although its precise function is yet to be clarified, CD20 is thought to play a role in B-cell development by mediating lipid raft-related signalling.[32] Our findings indicate that BAFF contributes to the regulation of B-cell development by modulating apoptotic elimination of B cells mediated by BCR and CD20. Furthermore, our results also indicate that BAFF can enhance cell proliferation in MLMA cells.

A number of studies have attempted to elucidate the molecular basis of the function of BAFF.[24,33–39] A major focus of recent investigations has been the pro-survival signalling of BAFF-R. Activation of the alternative NF-κB pathway (processing of NF-κB2 and the nuclear translocation of p52/RelB heterodimers) is a major outcome of BAFF-R-stimulation,[2,24,36] whereas BAFF-R also weakly activates the classical NF-κB pathway mediated by NF-κB1 and low-level nuclear translocation of p50/RelA DNA-binding activity is induced. Coincident with previous reports, we also observed that BAFF induced cleavage of both NF-κB2 and NF-κB1 in MLMA cells (Fig. 4). APRIL only activates NF-κB1 via either BCMA or TACI and did not inhibit CD20- and BCR-mediated apoptosis in MLMA cells, so the anti-apoptotic effect of BAFF is thought to be mediated mainly by NF-κB2 activation.

Recent studies have shown that NF-κB directly binds to the promoter region of the Bcl-2 gene and induces transcriptional activation.[39] Since Bcl-2 has an anti-apoptotic function, the elevated level of Bcl-2 protein is thought to be important for BAFF-mediated B-cell survival. In addition, BAFF is reported to temporarily inactivate GSK-3β via AKT-mediated phosphorylation.[34] Since GSK-3β has been found to cause apoptosis by inducing the degradation of Mcl-1 (an anti-apoptotic Bcl-2 family member) and compromising mitochondrial membrane integrity,[40] the BAFF-mediated phosphorylation of GSK-3β is thought to also participate in the anti-apoptotic effect of BAFF. Consistent with previous reports, we observed that BAFF treatment also induced both an increase in Bcl-2 expression and the transient phosphorylation of GSK-3β in MLMA cells. Therefore, it is likely that the inhibitory effect of BAFF against apoptosis mediated by CD20 or BCR is also mainly the result of NF-κB2-mediated Bcl-2 expression and the transient inactivation of GSK-3β.

The pro-apoptotic BH3-only Bcl-2 family member Bim was shown to sequestrate Bcl-2 and play an essential role for BCR cross-linking-induced apoptosis.[41] Moreover, Mcl-1 was shown to inhibit Bim selectively and to be essential both early in lymphoid development and later on in the maintenance of mature B lymphocytes.[42] Therefore, future investigation of the involvement of Bim and MCL-1 in the BAFF-induced inhibition of CD20-mediated and BCR-mediated apoptosis in MLMA cells should be interesting.

Interestingly, our findings indicated that BAFF treatment also induces the expression of a series of genes related to cell survival. For example, both the microarray analysis and the flow cytometric analysis revealed increased expression of CD40 after the treatment. Since CD40 is known to mediate pro-survival signalling upon interaction with CD40L expressed on activated T cells,[43] it is suggested that BAFF-mediated up-regulation of CD40 expression also contributes to B-cell survival *in vivo*. Indeed, we observed in this study that simultaneous stimulation with CD40 and BAFF resulted in better inhibition of BCR-induced and CD20-induced apoptosis than stimulation with by each of them alone. Therefore, it may be possible that BAFF-mediated up-regulation of CD40 inhibits apoptosis induction synergistically with the effect of BAFF *in vivo*.

The microarray analysis also revealed up-regulation of several genes involved in either the inhibition of apoptosis or the proliferation of B cells (Table 1). For example, Myb has been demonstrated to directly up-regulate Bcl-2 and suppresses apoptosis.[44,45] EBI3 is a subunit of interleukin-27 that increases proliferation of B cells.[46] CFLAR is known to inhibit the activation of caspase 8.[47] Therefore, our data may indicate that mechanisms other than NF-κB2-mediated Bcl-2 up-regulation are involved in the anti-apoptotic effect of BAFF in MLMA cells. Furthermore, because direct cross-talk between the BCR-signalling and BAFF-signalling systems has been reported,[48] BAFF-mediated signals may also be able to directly influence the BCR-mediated apoptotic signalling system.

It is well documented that BAFF-mediated signalling is involved in the survival of malignant B cells.[2,49] For example, BAFF is reported to be an autocrine pro-survival and proliferation factor for B-cell chronic lymphocytic leukaemia and multiple myeloma.[2,49–51] BAFF is also thought to promote cell survival and proliferation in Hodgkin and non-Hodgkin lymphoma. Therefore, BAFF and BAFF-R might be potential molecular targets in the treatment of B-cell malignancies.[52–54] Using a combination of blocking of BAFF-signalling and activation of apoptosis induction, such as CD20 cross-linking, a novel therapeutic approach would be developed.

In conclusion, BAFF-mediated signalling inhibited CD20-mediated or BCR-mediated apoptosis in MLMA cells. Although more detailed experiments are clearly needed, MLMA cells should provide a model for investigating the molecular basis of BAFF's effect on B cells *in vitro* and will help to elucidate how B cells survive in an immune system in which BAFF-mediated signalling is involved.

Acknowledgements

We thank S. Yamauchi for excellent secretarial work. This work was supported by a grant from the Japan Health Sciences Foundation for Research on Publicly Essential Drugs and Medical Devices (KHA1004), Health and Labour Sciences Research Grants (the third term comprehensive 10-year-strategy for cancer control H19-010, Research on Children and Families H18-005 and H19-003, Research on Human Genome Tailor made and Research on Publicly Essential Drugs and Medical Devices H18-005), and a Grant for Child Health and Development from the Ministry of Health, Labour and Welfare of Japan. It was also supported by CREST, JST, and the Budget for Nuclear Research of the Ministry of Education, Culture, Sports, Science and Technology, based on screening and counselling by the Atomic Energy Commission.

References

1 Plas DR, Rathmell JC, Thompson CB. Homeostatic control of lymphocyte survival: potential origins and implications. *Nat Immunol* 2002; **3**:515–21.

2 Mackay F, Silveira PA, Brink R. B cells and the BAFF/APRIL axis: fast-forward on autoimmunity and signaling. *Curr Opin Immunol* 2007; **19**:327–36.

3 Schneider P, MacKay F, Steiner V *et al.* BAFF, a novel ligand of the tumor necrosis factor family, stimulates B cell growth. *J Exp Med* 1999; **189**:1747–56.

4 Shu HB, Hu WH, Johnson H. TALL-1 is a novel member of the TNFfamily that is down-regulated by mitogens. *J Leukoc Biol* 1999; **65**:680–3.

5 Mukhopadhyay A, Ni J, Zhai Y, Yu GL, Aggarwal BB. Identification and characterization of a novel cytokine, THANK, a TNF homologue that activates apoptosis, nuclear factor-κB, and c-Jun NH_2-terminal kinase. *J Biol Chem* 1999; **274**:15978–81.

6 Moore PA, Belvedere O, Orr A *et al.* BLyS: member of the tumor necrosis factor family and B lymphocyte stimulator. *Science* 1999; **285**:260–3.

7 Gross JA, Johnston J, Mudri S *et al.* TACI and BCMA are receptors for a TNF homologue implicated in B-cell autoimmune disease. *Nature* 2000; **404**:995–9.

8 Mackay F, Woodcock SA, Lawton P, Ambrose C, Baetscher M, Schneider P, Tschopp J, Browning JL. Mice transgenic for BAFF develop lymphocytic disorders along with autoimmune manifestations. *J Exp Med* 1999; **190**:1697–710.

9 Khare SD, Sarosi I, Xia XZ *et al.* Severe B cell hyperplasia and autoimmune disease in TALL-1 transgenic mice. *Proc Natl Acad Sci USA* 2000; **97**:3370–5.

10 Schiemann B, Gommerman JL, Vora K, Cachero TG, Shulga-Morskaya S, Dobles M, Frew E, Scott ML. An essential role for BAFF in the normal development of B cells through a BCMA-independent pathway. *Science* 2001; **293**:2111–4.

11 Gross JA, Dillon SR, Mudri S *et al.* TACI-Ig neutralizes molecules critical for B cell development and autoimmune disease. Impaired B cell maturation in mice lacking BLyS. *Immunity* 2001; **15**:289–302.

12 Vora KA, Wang LC, Rao SP *et al.* Cutting edge: germinal centers formed in the absence of B cell-activating factor belonging to the TNF family exhibit impaired maturation and function. *J Immunol* 2003; **171**:547–51.

13 Schneider P. The role of APRIL and BAFF in lymphocyte activation. *Curr Opin Immunol* 2005; **17**:282–9.

14 Smith SH, Cancro MP. Cutting edge: B cell receptor signals regulate BLyS receptor levels in mature B cells and their immediate progenitors. *J Immunol* 2003; **170**:5820–3.

15 Ng LG, Sutherland AP, Newton R *et al.* B cell-activating factor belonging to the TNF family (BAFF)-R is the principal BAFF receptor facilitating BAFF costimulation of circulating T and B cells. *J Immunol* 2004; **173**:807–17.

16 Mackay F, Leung H. The role of the BAFF/APRIL system on T cell function. *Semin Immunol* 2006; **18**:284–9.

17 Thompson JS, Schneider P, Kalled SL *et al.* BAFF binds to the tumor necrosis factor receptor-like molecule B cell maturation antigen and is important for maintaining the peripheral B cell population. *J Exp Med* 2000; **192**:129–35.

18 Xia XZ, Treanor J, Senaldi G *et al.* TACI is a TRAF-interacting receptor for TALL-1, a tumor necrosis factor family member involved in B cell regulation. *J Exp Med* 2000; **192**:137–43.

19 Marsters SA, Yan M, Pitti RM, Haas PE, Dixit VM, Ashkenazi A. Interaction of the TNF homologues BLyS and APRIL with the TNFreceptor homologues BCMA and TACI. *Curr Biol* 2000; **10**:785–8.

20 Shu HB, Johnson H. B cell maturation protein is a receptor for the tumor necrosis factor family member TALL-1. *Proc Natl Acad Sci USA* 2000; **97**:9156–61.

21 Wu Y, Bressette D, Carrell JA *et al.* Tumor necrosis factor (TNF) receptor superfamily member TACI is a high affinity receptor for TNF family members APRIL and BLyS. *J Biol Chem* 2000; **275**:35478–85.

22 Thompson JS, Bixler SA, Qian F *et al.* BAFF-R, a newly identified TNF receptor that specifically interacts with BAFF. *Science* 2001; **293**:2108–11.

23 Gras MP, Laabi Y, Linares-Cruz G *et al.* BCMAp: an integral membrane protein in the Golgi apparatus of human mature B lymphocytes. *Int Immunol* 1995; **7**:1093–106.

24 Kayagaki N, Yan M, Seshasayee D *et al.* BAFF/BLyS receptor 3 binds the B cell survival factor BAFF ligand through a discrete surface loop and promotes processing of NF-κB2. *Immunity* 2002; **10**:515–24.

25 Chaouchi N, Vazquez A, Galanaud P, Leprince C. B cell antigen receptor-mediated apoptosis. Importance of accessory molecules CD19 and CD22, and of surface IgM crosslinking. *J Immunol* 1995; **154**:3096–104.

26 Shan D, Ledbetter JA, Press OW. Apoptosis of malignant human B cells by ligation of CD20 with monoclonal antibodies. *Blood* 1998; **91**:1644–52.

27 Kiyokawa N, Kokai Y, Ishimoto K, Fujita H, Fujimoto JHata JI. Characterization of the common acute lymphoblastic leukaemia antigen (CD10) as an activation molecule on mature human B cells. *Clin Exp Immunol* 1990; **79**:322–7.

28 Takenouchi H, Kiyokawa N, Taguchi T, Matsui J, Katagiri YU, Okita H, Okuda K, Fujimoto J. Shiga toxin binding to globotriaosyl ceramide induces intracellular signals that mediate cytoskeleton remodeling in human renal carcinoma-derived cells. *J Cell Sci* 2004; **117**:3911–22.

29 Kiyokawa N, Lee EK, Karunagaran D, Lin SY, Hung MC. Mitosis-specific negative regulation of epidermal growth factor receptor, triggered by a decrease in ligand binding and dimerization, can be overcome by overexpression of receptor. *J Biol Chem* 1997; **272**:18656–65.

30 Mimori K, Kiyokawa N, Taguchi T *et al.* Costimulatory signals distinctively affect CD20- and B-cell-antigen-receptor-mediated apoptosis in Burkitt's lymphoma/leukemia cells. *Leukemia* 2003; **17**:1164–74.

31 Levine MH, Haberman AM, Sant'Angelo DB, Hannum LG, Cancro MP, Janeway CA Jr, Shlomchik MJ. A B-cell receptor-specific selection step governs immature to mature B cell differentiation. *Proc Natl Acad Sci USA* 2000; **97**:2743–8.

32 Deans JP, Li H, Polyak MJ. CD20-mediated apoptosis: signalling through lipid rafts. *Immunology* 2002; **107**:176–82.

33 Enzler T, Bonizzi G, Silverman GJ, Otero DC, Widhopf GF, Anzelon-Mills A, Rickert RC, Karin M. Alternative and classical NF-κB signaling retain autoreactive B cells in the splenic marginal zone and result in lupus-like disease. *Immunity* 2006; **25**:403–15.

34 Patke A, Mecklenbrauker I, Erdjument-Bromage H, Tempst P, Tarakhovsky A. BAFF controls B cell metabolic fitness through a PKCb- and Akt-dependent mechanism. *J Exp Med* 2006; **203**: 2551–62.

35 Qian Y, Qin J, Cui G *et al.* Act1, a negative regulator in CD40- and BAFF-mediated B cell survival. *Curr Opin Immunol* 2007; **19**:327–36.

36 Claudio E, Brown K, Park S, Wang H, Siebenlist U. BAFF-induced NEMO-independent processing of NF-κB2 in maturing B cells. *Nat Immunol* 2002; **3**:958–65.

37 Craxton A, Draves KE, Gruppi A, Clark EA. BAFF regulates B cell survival by downregulating the BH3-only family member Bim via the ERK pathway. *J Exp Med* 2005; **202**:1363–74.

38 Mecklenbräuker I, Kalled SL, Leitges M, Mackay F, Tarakhovsky A. Regulation of B-cell survival by BAFF-dependent PKCdelta-mediated nuclear signaling. *Nature* 2004; **431**:456–61.

39 Viatour P, Beitires AM, Chariot A, Deregowski V, Leval L, Merville MP, Bours V. NF-κB2/p100 induces Bcl-2 expression. *Leukemia* 2003; **17**:1349–56.

40 Maurer U, Charvet C, Wagman AS, Dejardin E, Green DR. Glycogen synthase kinase-3 regulates mitochondrial outer membrane permeabilization and apoptosis by destabilization of MCL-1. *Mol Cell* 2006; **21**:749–60.

41 Enders A, Bouillet P, Puthalakath H, Xu Y, Tarlinton DM, Strasser A. Loss of the pro-apoptotic BH3-only Bcl-2 family member Bim inhibits BCR stimulation-induced apoptosis and deletion of autoreactive B cells. *J Exp Med* 2003; **198**:1119–26.

42 Opferman JT, Letai A, Beard Csorcinelli MD, Ong CC, Korsmeyer SJ. Development and maintenance of B and T lymphocytes requires antiapoptotic MCL-1. *Nature* 2003; **426**:671–6.

43 Kehry MR. CD40-mediated signaling in B cells. Balancing cell survival, growth, and death. *J Immunol* 1996; **156**:2345–8.

44 Taylor D, Badiani P, Weston K. A dominant interfering Myb mutant causes apoptosis in T cells. *Genes Dev* 1996; **10**:2732–44.

45 Frampton J, Ramqvist T, Graf T. v-Myb of E26 leukemia virus up-regulates bcl-2 and suppresses apoptosis in myeloid cells. *Genes Dev* 1996; **10**:2720–31.

46 Larousserie F, Charlot P, Bardel E, Froger J, Kastelein RA, Devergne O. Differential effects of IL-27 on human B cell subsets. *J Immunol* 2006; **176**:5890–7.

47 Chandrasekaran Y, McKee CM, Ye Y, Richburg JH. Influence of TRP53 status on FAS membrane localization, CFLAR (c-FLIP) ubiquitinylation, and sensitivity of GC-2spd (ts) cells to undergo FAS-mediated apoptosis. *Biol Reprod* 2006; **74**:560–8.

48 Patke A, Mecklenbrauker I, Tarakhovsky A. Survival signaling in resting B cells. *Curr Opin Immunol* 2004; **16**:251–5.

49 Haiat S, Billard C, Quiney C, Ajchenbaum-Cymbalista F, Kolb JP. Role of BAFF and APRIL in human B-cell chronic lymphocytic leukaemia. *Immunology* 2006; **118**:281–92.

50 Novak AJ, Darce JR, Arendt BK *et al.* Expression of BCMA, TACI, and BAFF-R in multiple myeloma: a mechanism for growth and survival. *Blood* 2004; **103**:689–94.

51 Moreaux J, Legouffe E, Jourdan E *et al.* BAFF and APRIL protect myeloma cells from apoptosis induced by interleukin 6 deprivation and dexamethasone. *Blood* 2004; **103**:3148–57.

52 Chiu A, Xu W, He B *et al.* Hodgkin lymphoma cells express TACI and BCMA receptors and generate survival and proliferation signals in response to BAFF and APRIL. *Blood* 2007; **109**:729–39.

53 He B, Chadburn A, Jou E, Schattner EJ, Knowles DM, Cerutti A. Lymphoma B cells evade apoptosis through the TNF family members BAFF/BLyS and APRIL. *J Immunol* 2004; **172**:3268–79.

54 Novak AJ, Grote DM, Stenson M *et al.* Expression of BLyS and its receptors in B-cell non-Hodgkin lymphoma: correlation with disease activity and patient outcome. *Blood* 2004; **104**:2247–53.

Original Paper

Acta Haematologica

Acta Haematol 827
DOI: 10.1159/000XXXXXX

Received: June 26, 2008
Accepted after revision: September 24, 2008
Published online: ■■■

Human Osteoblasts Support Hematopoietic Cell Development in vitro

Yusuke Shiozawa[a, b] Hisami Takenouchi[a] Tomoko Taguchi[a] Masahiro Saito[b] Yohko U. Katagiri[a] Hajime Okita[a] Toshiaki Shimizu[b] Yuichiro Yamashiro[b] Junichiro Fujimoto[a] Nobutaka Kiyokawa[a]

[a]Department of Developmental Biology, National Research Institute for Child Health and Development, and [b]Department of Pediatrics and Adolescent Medicine, Juntendo University School of Medicine, Tokyo, Japan

Key Words
Cell adhesion molecule · Cell signaling · Cytokines · Hematopoiesis · Osteoblasts · Stem cell factor

Abstract
Background/Aim: Although osteoblasts are thought to be the major component of the hematopoietic stem cell niche in the bone marrow microenvironment, the role of osteoblasts in hematopoiesis is still unclear. The ability of human osteoblasts to support early hematopoiesis was investigated. ***Methods and Results:*** Human CD34+ bone marrow cells cultured on human osteoblasts were capable of surviving without addition of cytokines and differentiated into myeloid cells with slight proliferation. The results of immunohistochemical experiments suggested activation of FAK and AKT in hematopoietic cells attached to osteoblasts. When stem cell factor, Flt3-L, and IL-3 were added to the coculture system, each cytokine distinctively enhanced proliferation and differentiation of CD34+ bone marrow cells. ***Conclusion:*** The results suggest that human osteoblasts have the ability to support hematopoietic cell development in vitro.

Introduction

Bone marrow stromal cells, including fibroblasts, adipocytes, macrophages, endothelial cells, and osteoblasts, have been ascribed an important role in hematopoiesis. In addition to the effect of cytokines secreted by stromal cells, direct contact between hematopoietic and stromal cells or extracellular matrix synthesized by bone marrow stromal cells has been implicated in the formation of various hematopoietic cells [1, 2]. Having the ability to self-renew in this environment, hematopoietic stem cells (HSCs) proliferate and differentiate into hematopoietic cells of various lineages, e.g. lymphocytes and myeloid cells.

HSCs are thought to be located in a specific stromal niche in the bone marrow for cell maintenance, proliferation and differentiation. Recent publications have highlighted that osteoblasts are the major component of the HSC niche in the bone marrow microenvironment [3–5]. Zhang et al. [3] presented osteoblasts as key components of the niche that supports HSC development, being functionally controlled via the bone morphogenetic protein signaling pathway. They also suggested that N-cadherin and β-catenin are responsible for the interaction between osteoblasts and long-term HSCs. Calvi et al. [4] demonstrated that osteoblasts are a regulatory com-

KARGER
Fax +41 61 306 12 34
E-Mail karger@karger.ch
www.karger.com

0001–5792/08/0000–0000$24.50/0

Accessible online at:
www.karger.com/aha

Nobutaka Kiyokawa, MD, PhD
Department of Developmental Biology
National Research Institute for Child Health and Development
2-10-1, Okura, Setagaya-ku, Tokyo 157-8535 (Japan)
Tel./Fax +81 3 3417 2496, E-Mail nkiyokawa@nch.go.jp

ponent of the HSC niche and control stem cell function through the Notch 1-Jagged 1 pathway. They further stated that parathyroid hormone affects the ability of osteoblasts to expand HSCs. Arai et al. [5] reported that the tight adhesion between HSCs and osteoblasts induced through the Tie2/Ang-1 signaling pathway plays an important role in the maintenance of HSCs in a quiescent state in the bone marrow niche. Despite these findings, however, the role of osteoblasts in hematopoiesis is still unclear.

In this study, we investigated the effect of a primary human osteoblast culture on proliferation and differentiation of human CD34+ bone marrow cells and found that human osteoblasts have the ability to maintain and support hematopoietic cell development in vitro. Primary human osteoblast cultures may provide an in vitro model for the hematopoietic microenvironment.

Materials and Methods

Recombinant human stem cell factor (SCF), human fms-like tyrosine kinase 3 ligand (Flt3-L), and human interleukin (IL)-3 were purchased from Pepro Tec (London, UK). All cytokines were dissolved in phosphate-buffered saline and diluted with culture medium to the concentration indicated. The following mouse monoclonal antibodies (mAbs) against human antigens were used: carboxyfluorescein succinimidylester (CFS)-conjugated anti-CD184 (CXCR4) from Dako Cytomation (Glostrup, Denmark), phycoerythrin- and allophycocyanin-conjugated anti-CD33, phycoerythrin-cyanine (PC) 5-conjugated anti-CD19, PC7-conjugated anti-CD34, allophycocyanin-conjugated anti-CD45, purified anti-CD29 (β_1-integrin), anti-CD49d (α_4-integrin), anti-CD106 (VCAM-1), and anti-fibronectin from Beckman/Coulter (Westbrook, Mass., USA), purified anti-CD166 (activated leukocyte cell adhesion molecule), anti-β-catenin, anti-N-cadherin, and anti-paxillin from Becton Dickinson Biosciences (San Diego, Calif., USA), anti-vinculin from Chemicon International (Temecula, Calif., USA), and anti-osteocalcin from Takara Bio (Shiga, Japan). Purified mAbs were labeled with the Zenon™ Alexa Fluor® 488 and 546 mouse IgG1 labeling kit according to the manufacturer's protocol (Invitrogen, Carlsbad, Calif., USA). The rabbit polyclonal Abs against phospho-specific AKT from Cell Signaling Technology (Beverly, Mass., USA) and phospho-specific FAK from Affinity BioReagents (Golden, Colo., USA) were also used. Unless otherwise indicated, all other chemical reagents were obtained from Wako Pure Chemical Industries (Osaka, Japan).

Human CD34+ bone marrow cells and a primary culture of human osteoblasts purchased from Cambrex Bio Science Walkersville (Walkersville, Md., USA) were used. The cells had been isolated from human tissue after obtaining informed consent from the donor and were maintained in RPMI 1640 medium (Sigma-Aldrich, St. Louis, Mo., USA) supplemented with 10% (v/v) fetal calf serum (Sigma-Aldrich) at 37°C under a humidified 5% CO_2 atmosphere. The primary culture of human osteoblasts was isolated from the spongy section of the bone head via an explant using the methods established by the provider. The provider confirmed that the majority of the cells were positive for alkaline phosphatase and bone mineralization (von Kossa stain), representing osteoblast phenotypes.

Cells from the primary culture of human osteoblasts were plated and grown to approximately three-fourth confluence on a 12-well tissue plate (Asahi Techno Glass, Chiba, Japan). The CD34+ cells were plated at a concentration of 4×10^4 cells/well/2 ml on the human osteoblasts in RPMI 1640 medium supplemented with 10% fetal calf serum, with and without cytokines. Each cytokine was added at a concentration of 100 ng/ml. After cultivation for the periods indicated, the cells were harvested with 0.25% trypsin plus 0.02% ethylenediamine tetraacetic acid (Immuno-Biological Laboratories, Gunma, Japan), and the number of cells per well was counted. All experiments were performed in triplicate, and cell numbers are reported as means ± SD. For the histological studies, cells were cultured on type-I collagen-coated coverslips (Asahi Techno Glass). At the end of the culture period, the cells on the coverslips were examined after either May-Grünwald-Giemsa staining or immunohistochemical staining.

RT-PCR was performed as described previously [6]. The primer sets used in this study are listed in table 1. The PCR products were separated on 1.5% agarose gel.

For immunostaining, coverslips were fixed with ice-cold acetone for 15 min, incubated with fluorescence-labeled mouse mAbs at room temperature for 30 min, and washed in phosphate-buffered saline. In case of the rabbit polyclonal Abs, secondary goat anti-rabbit IgG Ab conjugated with Alexa Fluor 546 (1:300 dilution, Invitrogen) was used for labeling. The cells were then stained with 4′,6-diamidino-2-phenylindole (200 ng/ml, Sigma-Aldrich) and Alexa Fluor 633-conjugated phalloidin (Invitrogen).

Confocal laser scanning was performed with a FV500 confocal laser scanning microscope (Olympus, Tokyo, Japan). A water immersion objective (×40, NA1.7) was used, and simultaneous multifluorescence acquisitions were performed with the 351- and 488-, 546-, and 633-nm laser lines to excite 4′,6-diamidino-2-phenylindole, Alexa Fluor 488, 546, and 633, respectively. Fluorescence images were selected using appropriate multifluorescence dichroic mirrors and band pass filters using the sequential acquisition mode.

A multicolor immunofluorescence study was performed using a combination of carboxyfluorescein succinimidylester, phycoerythrin, PC-5, and PC-7. Cells were stained with fluorescence-labeled mAbs and analyzed by flow cytometry (EPICS-XL, Beckman/Coulter), as described previously [7]. The gates were set to exclude dead cells and osteoblasts, and 1×10^4 gated cells were analyzed. Data are displayed as histograms of log-fluorescence intensity versus log-fluorescence intensity.

Results

As described in Materials and Methods, the primary culture of human osteoblasts used in this study was qualified and confirmed by the provider, i.e. that the majority of the cells represent osteoblast phenotypes. Using im-

Table 1. Primer sequences

Primer		Sequence	Product size, bp
IL-1α	Sense	5′-TGCTGCATTACATAATCTGG-3′	738
	Anti-sense	5′-TCATGAAATCCTAGGTCTGT-3′	
IL-1β	Sense	5′-CTGGAGAGTGTGATCCCAA-3′	212
	Anti-sense	5′-GACACAAATTGCATGGTGAA-3′	
IL-3	Sense	5′-ACCTTCGAAGGCCAAACCTG-3′	271
	Anti-sense	5′-AGAGAACGAGCTGGACGTTG-3′	
IL-6	Sense	5′-GAGTACAAAAGTCCTGATCC -3′	587
	Anti-sense	5′-TATTTGAGGTAAGCCTACAC-3′	
IL-7	Sense	5′-AAAGTTTCAGAAGGCACAAC-3′	314
	Anti-sense	5′-CTAGGAAGCATTCCACTCTG-3′	
IL-9	Sense	5′-TCTCAGATGACCAATACCAC-3′	216
	Anti-sense	5′-TCATATCTTGCCTCTCATCC-3′	
G-CSF	Sense	5′-ATAGCGGCCTTTTCCTCTAC-3′	863
	Anti-sense	5′-TGATGTTCGGGAGTCAAACC-3′	
M-CSF	Sense	5′-GCAACTGCCTGTACCCCAAA-3′	614
	Anti-sense	5′-CTGAGCAGGGCAGATGGATG-3′	
GM-CSF	Sense	5′-AGCATGTGAATGCCATCCAG-3′	434
	Anti-sense	5′-TTGGTCCCTCCAAGATGACC-3′	
Flt3-L	Sense	5′-TGGATGGAGCGGCTCAAGAC-3′	136
	Anti-sense	5′-TGTTGGTCTGGACGAAGCGA-3′	
LIF	Sense	5′-GCTGTTGGTTCTGCACTGGA-3′	621
	Anti-sense	5′-ACTCCTGAGATCCCTCGGTT-3′	
OPG	Sense	5′-AGATCCTGAAGCTGCTCAGT-3′	319
	Anti-sense	5′-AAAGCCTCAAGTGCCTGAGA-3′	
SCF	Sense	5′-ACAGCTTGACTGATCTTCTG-3′	711
	Anti-sense	5′-TTGTAAGACTTGGCTGTCTC-3′	
SDF-1α	Sense	5′-ATTCAGGAGTACCTGGAGAA-3′	522
	Anti-sense	5′-CAGTGTCTGAAGAAAGGACA-3′	
VEGF	Sense	5′-CTACCTCCACCATGCCAAGT-3′	577
	Anti-sense	5′-AGATCTGGTTCCCGAAACCC-3′	
CD166	Sense	5′-GTATTCCAGAACACGATGAG-3′	272
	Anti-sense	5′-TATCTCTGGACAACTAGGAC-3′	
Fibronectin	Sense	5′-GGATGACTCGTGCTTTGACC-3′	321
	Anti-sense	5′-TGCCACTGTTCTCCTACGTG-3′	
N-cadherin	Sense	5′-GTGCTGATGTTTGTGGTATG-3′	514
	Anti-sense	5′-CTGAAGTTCAGTCATCACCT-3′	
Jagged-1	Sense	5′-CAGGACCTGGTTAACGGATT-3′	936
	Anti-sense	5′-CGTTTCTACAAGGGTTGCTC-3′	
GAPDH	Sense	5′-CCACCCATGGCAAATTCCATGGCA-3′	598
	Anti-sense	5′-TCTAGACGGCAGGTCAGGTCCACC-3′	

munohistochemical staining, the majority of cells were positive for osteocalcin (fig. 1a), an osteoblast-specific protein, indicating that the cells indeed possess the characteristics of osteoblast.

First, we investigated the expression of adhesion-related molecules in the osteoblasts by immunohistostaining. As shown in figure 1b, filamentous distribution of CD106 was detected by confocal microscopy. Fibronectin was also expressed in the form of filaments around the cells, but occasionally it was distributed in the form of coarse bundles (arrowhead). Expression of the protein N-cadherin in the form of a fine mesh was also detected by immunohistostaining (fig. 1b). We also detected mRNA expression of adhesion-related molecules CD166,

fibronectin, N-cadherin, and Jagged-1 in the osteoblasts (fig. 1c).

Next, we characterized cytokine expression of cells in the primary culture of human osteoblasts. RT-PCR revealed mRNA expression of cytokines, including IL-1β, IL-6, Flt3-L, leukemia inhibitory factor (LIF), osteoprotegrin (OPG), stromal cell-derived factor (SDF-1α), and vascular endothelial growth factor (VEGF), in osteoblasts (fig. 1c). No expression of other cytokines, i.e. IL-1α, IL-3, IL-7, IL-9, granulocyte colony-stimulating factor (G-CSF), macrophage colony-stimulating factor (M-CSF), granulocyte macrophage colony-stimulating factor (GM-CSF), or SCF, was detected under the same conditions (fig. 1c).

To investigate the effect of human osteoblasts on hematopoiesis in vitro, we cultured human CD34+ bone marrow cells on cells from the primary culture of the human osteoblasts. When human CD34+ bone marrow cells were cultured alone in the absence of cytokine addition, they almost all died (fig. 2). By contrast, the human CD34+ bone marrow cells were maintained and proliferated slightly on human osteoblasts in the absence of cytokine supplementation. As shown in figure 2, part of the hematopoietic cells adhered to osteoblasts, forming a small colony, whereas another part of hematopoietic cells floated (data not shown). The culture initially contained 40,000 human CD34+ bone marrow cells, 2 and 4 weeks later 40,000–160,000 and 120,000–270,000 hematopoietic cells were collected, respectively.

We analyzed the subsets of the hematopoietic cells that had survived on the osteoblasts by flow cytometry. When examined after 2 weeks of coculture, the majority of hematopoietic cells were CD33+ myeloid cells (fig. 3). In addition, the human osteoblasts had the ability to maintain a few human CD34+ bone marrow cells (fig. 3), and a small amount of hematopoietic cells still remained to express CD34 after 2 weeks of coculture.

It is noteworthy that occasionally proliferation of CD19+ B-lineage cells on osteoblasts was observed, and one experiment revealed that 46.2 and 13.0% of the hematopoietic cells were B-lineage cells after 2 and 4 weeks of coculture, for example (data not shown). However, the proliferation of B-lineage cells seems to be dependent on the lot of human CD34+ bone marrow cells. Since CD34+ bone marrow cells contained a sizable population of CD19+CD34+ cells in those cases (data not shown), it is most likely that osteoblasts can maintain the B-lineage-committed cells rather than promote B-cell differentiation.

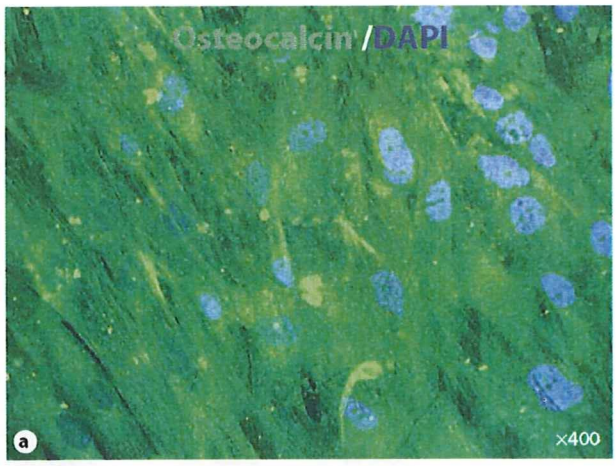

Fig. 1. Expression of osteocalcin and cell adhesion molecules in a primary culture of osteoblasts detected by immunohistochemistry. **a** Osteoblast primary culture grown on coverslips was stained with fluorescein-labeled antibodies to the osteocalcin and examined by confocal microscopy.

Next, we investigated the effect of addition of cytokines, including SCF, Flt3-L and IL-3, on the growth and differentiation of human CD34+ bone marrow cells cultured on human osteoblasts. In the absence of osteoblasts, SCF and IL-3 differently supported the proliferation of hematopoietic cells and 180,000 ± 42,426 and 1,295,000 ± 49,497 cells had grown after a 2-week cocultivation from an initial 40,000 CD34+ bone marrow cells, respectively (fig. 3b). By contrast, Flt3-L induced no significant proliferation of hematopoietic cells (fig. 3b).

In the presence of osteoblasts, however, the subsequent hematopoietic cell number was significantly increased compared with hematopoietic cells cultured with cytokine alone. When 55,000 ± 21,213 hematopoietic cells had grown from an initial 40,000 CD34+ bone marrow cells after a 2-week cocultivation on human normal osteoblasts, cytokines SCF, Flt3-L, and IL-3 markedly increased hematopoietic cell recovery to 990,000 ± 183,848, 355,000 ± 77,782, and 2,370,000 ± 367,696, respectively (fig. 3c). In each case, the majority of cells were CD33+ (fig. 3c). An especially remarkable increase in the CD34+ cell number was achieved with the combination of osteoblasts and IL-3 (fig. 3d).

We further investigated the effect of other factors which may affect either osteoblasts or CD34+ bone marrow cells, including parathyroid hormone, vitamin D, MIP-1α, BMP-2, IL-7, and LIF, whereas no significant ef-

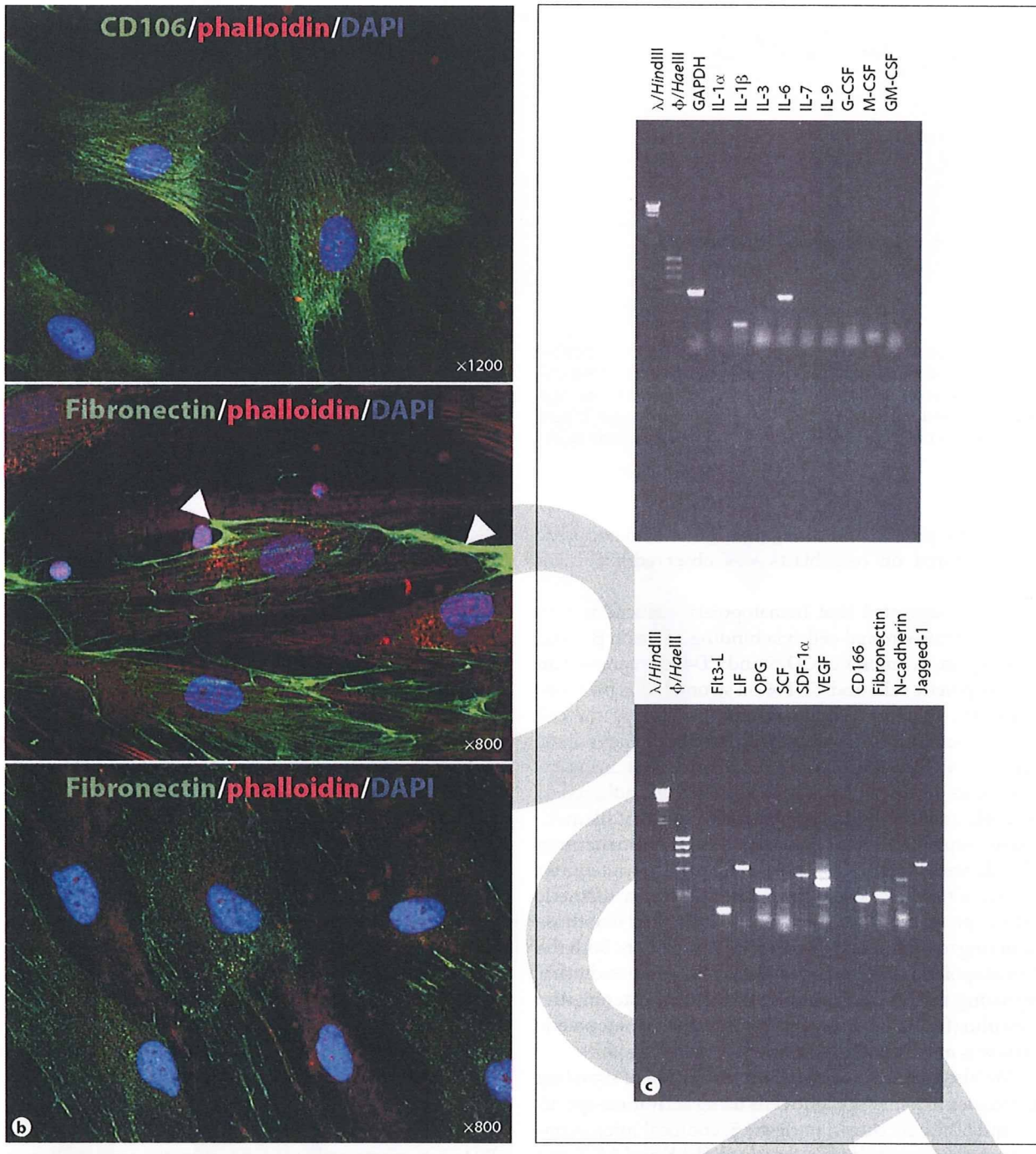

Fig. 1. b The same samples were stained with fluorescein-labeled antibodies to the cell adhesion molecules indicated and examined by confocal microscopy. **c** Expression of cytokines and cell adhesion molecules in osteoblasts detected by RT-PCR. To investigate mRNA expression of the cytokines and cell adhesion molecules indicated, total RNAs were extracted from a primary culture of human osteoblasts and RT-PCR analysis was performed. The PCR products obtained were subjected to electrophoresis with molecular weight markers ϕ/X174/*Hae*III and λ/*Hin*dIII.

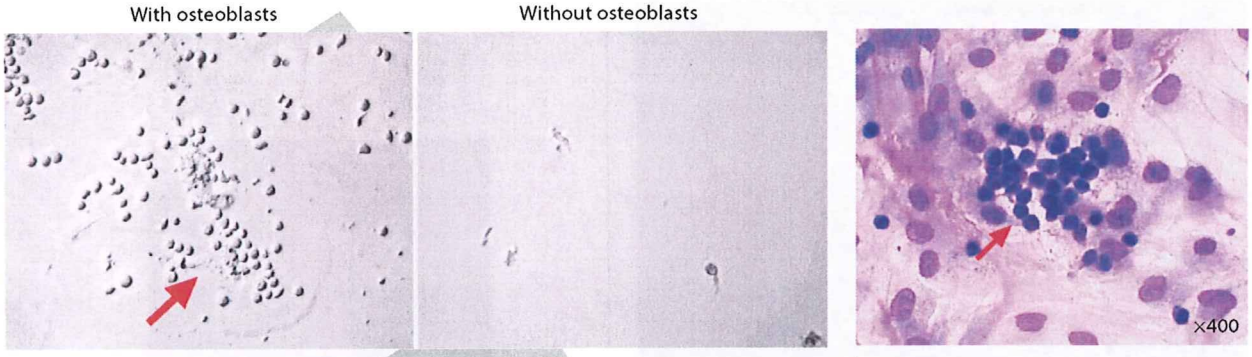

Fig. 2. Human CD34+ bone marrow cells grown on osteoblast primary cultures. **a** Human CD34+ bone marrow cells were cultured for 2 weeks on osteoblast primary cultures grown on coverslips and examined by phase-contrast microscopy (magnification ×100). **b** After May-Grünwald-Giemsa staining, cells were examined by light microscopy. The small nuclear cells gathered at the center are human CD34+ bone marrow cells (arrow), and the large nuclear cells present at the circumference are human osteoblasts (magnification ×400).

fect on the growth and differentiation of hematopoietic cells cultured on osteoblasts was observed (data not shown).

It was suggested that hematopoietic cells adhere to bone marrow stromal cells via binding between β_1- and α_4-integrin, a complex of CD29 and CD49d, expressed on hematopoietic cells and CD106 on stromal cells [8]. Consequently, the intracellular signaling required for cell survival and maintenance was initiated in hematopoietic cells [9]. As shown in figure 4, immunohistostaining experiments revealed that hematopoietic cells adhered to osteoblasts as they got twisted to the CD106 that filamentously expressed on osteoblasts. Immunohistostaining also showed that the CD166 staining pattern was similar to that of fibronectin and that some of the hematopoietic cells expressed CD166, and those cells looked like those adhering to osteoblasts that also express CD166. Both the hematopoietic cells and osteoblasts also expressed other signaling molecules, including paxillin, β-catenin, and vinculin (fig. 4). Paxillin expression in the hematopoietic cells was much greater than in osteoblasts (fig. 4).

We also investigated the phosphorylation of signaling molecules in hematopoietic cells using activation-specific antibodies. As shown in figure 5, confocal microscopic analysis showed phosphorylation of FAK and AKT, and there was clear colocalization of phosphorylated FAK and AKT with CD49d and CD29, respectively (fig. 5, bottom panels).

Thus, we tested the effect of cell adhesion mediated by CD29 and CD49d on the maintenance of hematopoietic cells on osteoblasts. When the anti-CD29 antibody that can interfere in the binding between CD29 and CD106 was added to the coculture of CD34+ bone marrow cells and osteoblasts, subsequent hematopoietic cell proliferation was clearly reduced (fig. 6). Identical results were observed for the anti-CD49d antibody (fig. 6).

Since CD184 (CXCR4) has been suggested to contribute to the homing of hematopoietic cells, we investigated the effect of osteoblasts on CD184 expression by hematopoietic cells. As shown in figure 7a, human CD34+ cells purified from bone marrow did not express CD184. When cultured on osteoblasts, however, expression of CD184 was significantly increased and the hematopoietic cells were divided into several fractions based on the diverse patterns of CD184 and CD33 co-expression (fig. 7).

In the absence of osteoblasts, on the other hand, each cytokine also induced CD184 expression by hematopoietic cells in a distinct manner (fig. 7). When CD34+ bone marrow cells were cultured in the presence of osteoblasts,

Fig. 3. Effect of human osteoblasts and cytokines on the growth and differentiation of human CD34+ bone marrow cells. Human CD34+ bone marrow cells were cultured with or without human osteoblasts (OB) for 2 weeks in the presence or absence of the cytokines indicated. After cultivation, the ensuing hematopoietic cells were collected, counted, and positivity for CD33 and CD34 was determined by flow cytometry. The actual total cell numbers and the numbers of cells in each subpopulation are represented by bar graphs.

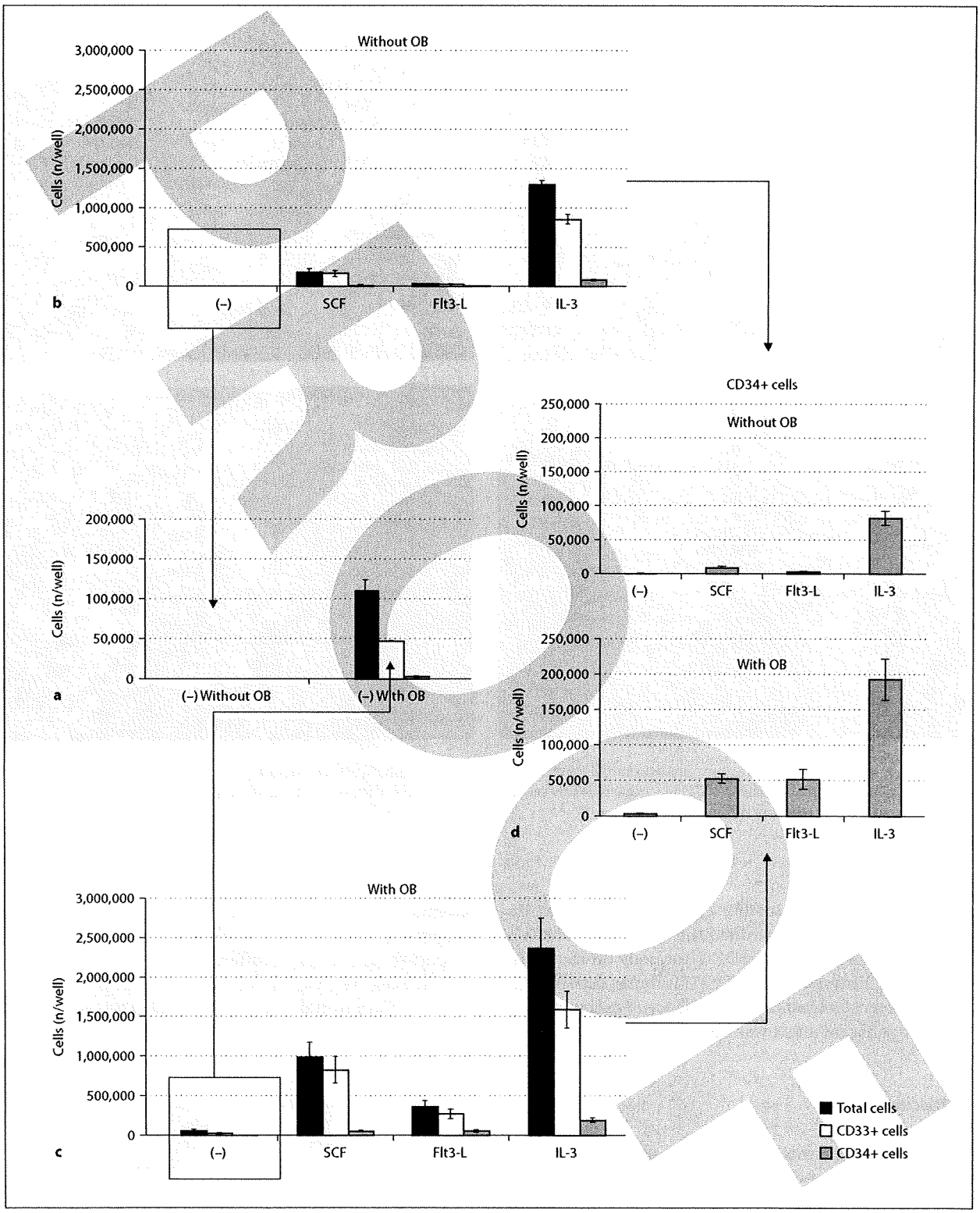

3

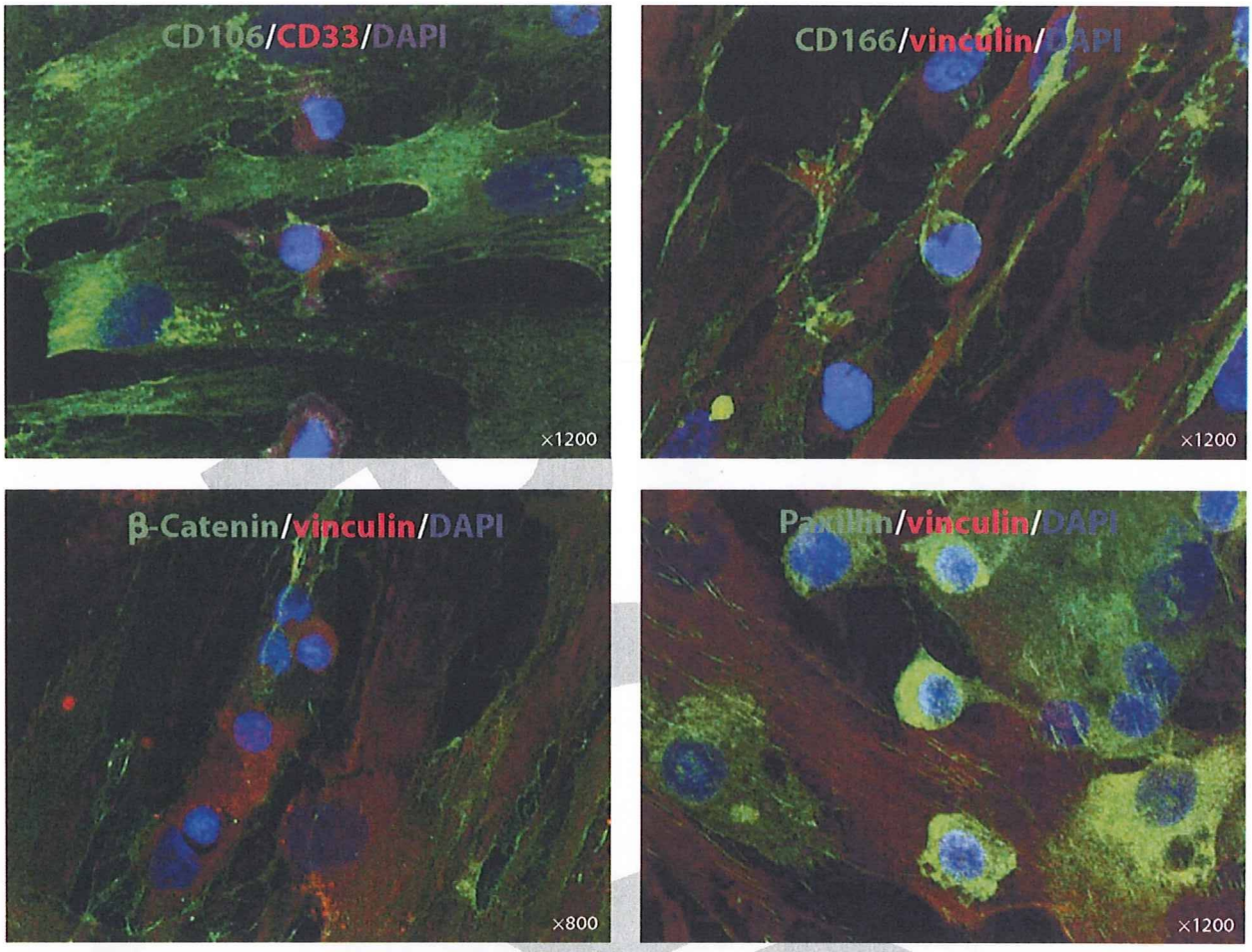

Fig. 4. Immunohistochemical analysis of the interaction between osteoblasts and human CD34+ bone marrow cells. Human CD34+ bone marrow cells were grown on a primary culture of osteoblasts for 2 weeks and examined as in figure 1b.

addition of cytokines further enhanced CD184 expression (fig. 7). We also examined the effect of SDF-1, a ligand for CD184, and anti-SDF-1 antibody on the proliferation and differentiation of CD34+ bone marrow cells cultured on osteoblasts in the presence of each cytokine, but no significant effect was observed (data not shown).

Discussion

As reported in this paper, when cultured on human osteoblasts, human CD34+ bone marrow cells were able to survive without the addition of any cytokine, and differentiated into myeloid cells with slight proliferation, suggesting that human osteoblasts possess the ability to support the survival and differentiation of hematopoietic cells in vitro. Analysis by confocal microscopy suggested that cell adhesion molecules, including CD29/49d, CD106,

Fig. 5. Phosphorylation of cell signaling molecules in hematopoietic cells cultured on osteoblasts detected by immunohistochemistry. **a** Human CD34+ bone marrow cells were grown on a primary culture of osteoblasts for 2 weeks and stained with the combination of phospho-specific antibodies and anti-cell adhesion molecule antibodies and examined as in **a**.

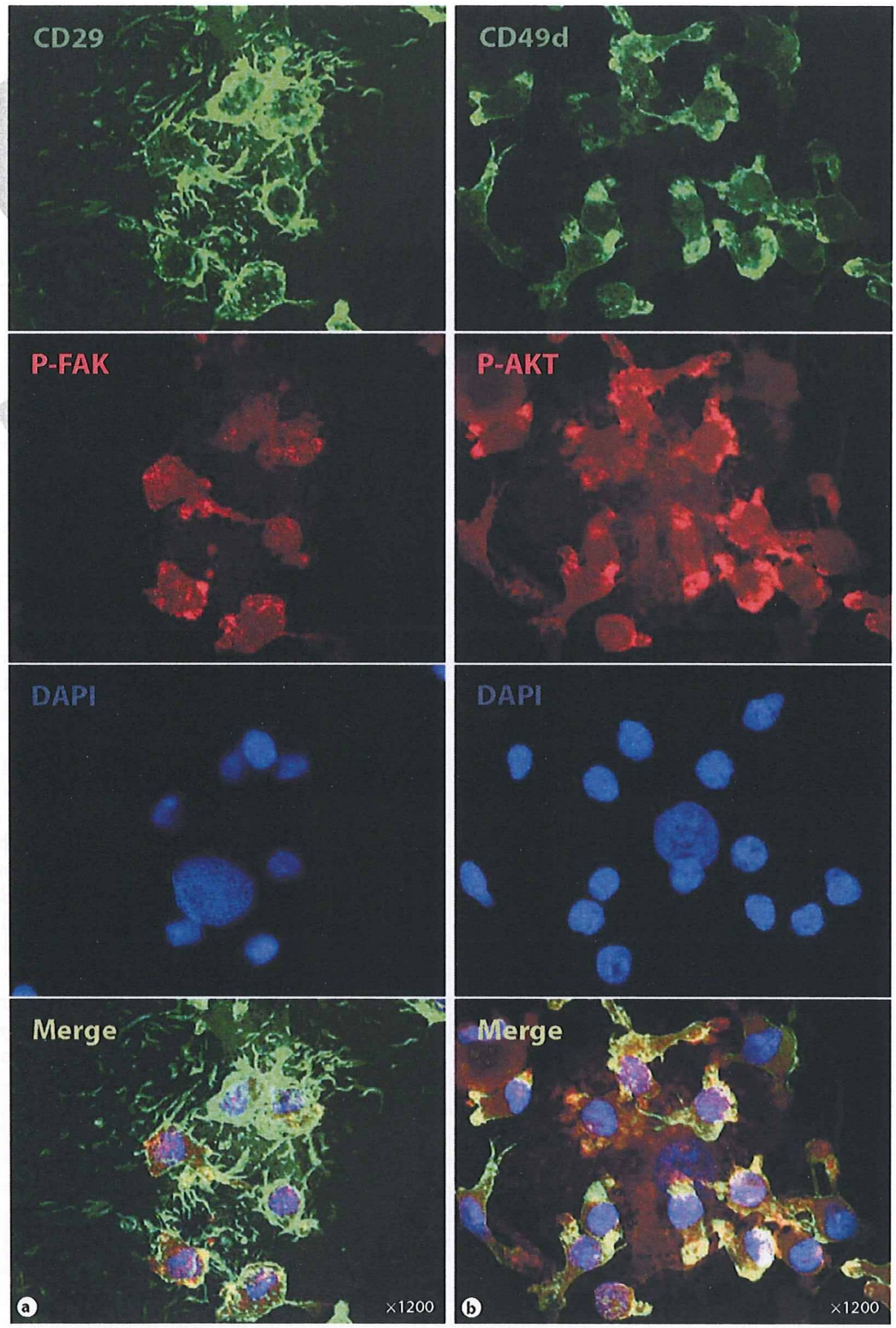

5